University of Chester

Author(s): Pedro M Lima; Neville J Ford; Patricia M Lumb

Title: Computational methods for a mathematical model of propagation of nerve impulses in myelinated axons

Date: 2014

Originally published in: Applied Numerical Mathematics

Example citation: Lima, P.M., Ford, N.J., & Lumb, P.M. (2014). Computational methods for a mathematical model of propagation of nerve impulses in myelinated axons. *Applied Numerical Mathematics*, *85*, 38–53. doi: http://dx.doi.org/10.1016/j.apnum.2014.06.004

Version of item: Author's post-print as accepted for publication

Available at: http://hdl.handle.net/10034/322541

Computational methods for a mathematical model of propagation of nerve impulses in myelinated axons

Pedro M. Lima[a,*], Neville J. Ford[b], Patricia M. Lumb[b]

[a]*CEMAT, Instituto Superior Técnico, Universidade de Lisboa, 1049-001 Lisboa, Portugal*
[b]*Dept. of Mathematics, University of Chester, CH1 4BJ, Chester, UK*

Abstract

This paper is concerned with the approximate solution of a nonlinear mixed type functional differential equation (MTFDE) arising from nerve conduction theory. The equation considered describes conduction in a myelinated nerve axon. We search for a monotone solution of the equation defined in the whole real axis, which tends to given values at $\pm\infty$. We introduce new numerical methods for the solution of the equation, analyse their performance, and present and discuss the results of the numerical simulations.

Keywords: Discrete FitzHugh-Nagumo equation, Mixed-type functional differential equation, method of steps, finite-difference method, Newton method, nerve conduction, myelinated axon.
2000 MSC: 34K06, 34K28, 65Q05, 34K10

1. Introduction

In 1952, A. Hodgkin and A. Huxley [11] introduced a mathematical model that describes the excitation and flow of electrical current through the surface of a giant nerve fibre from a squid. This model (usually known as the HH-model) consists of a system of four ordinary differential equations with four unknowns (the state variables V, m, h, n), of which V is the membrane potential difference and the remainder are conductance variables. An extensive mathematical analysis of this model has been carried out by R. FitzHugh [8], [9]. In order to explain the main features of the HH-model, R. FitzHugh reduced it to a system of two ODES, still conserving the main properties of the original system. The reduced system, which he called the Bonhoeffer-Van der Pol (BVP) model, has the form:

$$\begin{cases} \frac{dx}{dt} = c(y + x - x^3/3 + z) \\ \frac{dy}{dt} = -(x - \alpha + \beta y)/c \end{cases},$$
(1)

where z is a known function (the so-called stimulus intensity, which corresponds to membrane current in the HH-model); α, β, c are constants satisfying

$$1 - \frac{2\beta}{3} < \alpha < 1, \quad 0 < \beta < 1, \quad \beta < c^2.$$
(2)

In the case $\alpha = \beta = z = 0$, system (1) reduces to the well-known Van der Pol equation. R. FitzHugh used phase space and stability theory to investigate the qualitative behaviour of system (1).

Comparing system (1) with the original HH-model, FitzHugh concluded that the HH variables V and m together behave like x, while h and n behave like y. He also says that "the coordinates x and y are not to be identified physically, except to say that x shares the properties of both membrane potential and excitability, while y is responsible for accommodation and refractoriness".

The study of nerve excitation and conduction has been continued by Nagumo and his co-authors [17], who made an active phase transmission line, using tunnel diodes, and simulated an animal nerve axon. These authors started by simulating electronically the behaviour of the HH and the FitzHugh models in the case of the "space clamp", that is, when the excitation of a nerve axon is spatially uniform. Then, in order to consider propagation of excitation, they considered x as a function of two variables s, t where s is the space variable. Following Hodgkin and Huxley, they assumed that the current intensity z in the first equation of the system (1) can be replaced by

$$ z(t) = \frac{1}{r} \frac{\partial^2 x}{\partial s^2}, $$

where r is a constant (depending from the axoplasmical resistance and membrane capacitance). In this case, from the system (1) one obtains the following system of partial differential equations:

$$ \begin{cases} \frac{1}{r} \frac{\partial^2 x}{\partial s^2} = \frac{1}{c} \frac{\partial x}{\partial t} - y - (x - x^3/3) \\ c \frac{\partial y}{\partial t} + \beta y = \alpha - x \end{cases}, \tag{3} $$

which are usually known as the FitzHugh-Nagumo equations.

In all the above-mentioned models of nerve excitation and propagation of electronic impulses, nerves are considered as electric cables, through which electric current flows. This is the case for the squid nerve, studied by Hodgkin and Huxley, but in other animals (like frogs, for example) nerve axons have a different structure. The nerve membrane is insulated by a substance called myelin (see fig. 1). According to Bell [3], " myelination of an axon allows it to conduct neuroelectric signals by exciting only a small portion of membrane exposed to the extracellular medium at the nodes of Ranvier. This permits transmission at greatly reduced energy expenditure and higher speeds than comparably sized unmyelinated axons". In models of myelinated axons, the following hypothesis is assumed: the myelin has such high resistance and low capacitance that it completely insulates the membrane (pure saltatory condition).

Under this hypothesis the nodes of Ranvier can be represented as active point sources of electric current. Moreover, basic transmission is accomplished by sufficiently stimulating a node so that its transmembrane potential reaches a certain threshold level. Then local ionic currents are generated which excite the neighbouring node enough to achieve the threshold potential. As a consequence, new local currents are generated at the neighbouring node and the process propagates across the nerve axon, giving the effect of excitation jumping from node to node.

As remarked by R. FitzHugh in [9], this case requires that the active membrane equations be solved at far fewer points along the fibre than does the case of a continuous axon. In the paper FitzHugh suggests that in the case of myelinated axons the HH equations are used to represent the membrane current only at the nodes. At other nerve points, nerve conduction is modelled just by an equation of the form:

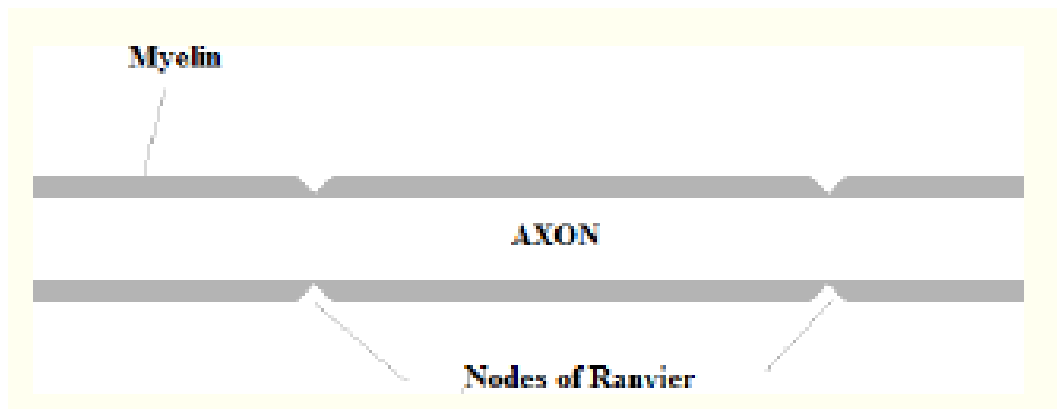$$ C \frac{\partial V}{\partial t} = \frac{\partial^2 V}{\partial x^2} - \frac{V}{r}, \tag{4} $$

Figure 1: Structure of a myelinated axon

where V is the membrane potential, C and r are constants.

This model yields a large system of equations: four ODEs at each node of Ranvier and the PDE (4). However, only the PDE (4) has to be solved in the whole axon, which makes the case of the myelinated axon more suitable for computation. This was remarked on by R. FitzHugh in 1962, when the potential computational possibilities were quite different from nowadays.

Modelling of impulse propagation in myelinated axons can be simplified if the nerve excitation at the nodes is represented by the system (1), instead of the HH equations. In this way J. Bell [3] obtained the following system of differential-difference equations:

$$\begin{cases} \frac{1}{R}(v_{k+1} - 2v_k + v_{k-1}) = C\frac{dv_k}{dt} - f(v_k) + w_k \\ \sigma v_k - \gamma w_k = \frac{dw_k}{dt} \end{cases} , \ k \in Z, \qquad (5)$$

where v_k and w_k are the potential and the recovery variables, respectively, at the $k-th$ node of Ranvier. σ and γ are non-negative rate constants, R and C are the axoplasmical resistance and the nodal membrane capacitance. The function f represents a current-voltage relation and is supposed to satisfy the following conditions:

$$f \in C^1([0, b]), \ f(0) = f(a) = f(1) = 0,$$
$$f(v) < 0, \ if \ 0 < v < a; \qquad (6)$$
$$f(v) > 0, \ if \ a < v < 1.$$

In [3] and [5] this function is taken as

$$f(v) = bv(v - a)(1 - v), \qquad (7)$$

where $b > 0$ and $a \in]0, 1[$ is the threshold potential . In this paper we will be concerned only with a function f of the type (7). According to [3] two basic properties of the myelinated axon are the following:

- it possesses threshold behaviour; this means that there are conditions which guarantee either the decay of a solution (subthreshold response) or non-decay of a solution (suprathreshold response);

- it is able to conduct pulses.

In order to study the threshold behaviour, the system (5) can be further simplified by neglecting the recovery process (that is, it is assumed that the constants σ and γ are so small that the recovery process has no

3

influence on any threshold condition). In this case, the system (5) reduces to the following equation:

$$\frac{1}{R}(v_{k+1} - 2v_k + v_{k-1}) + f(v_k) = C\frac{dv_k}{dt}, \qquad k \in Z. \tag{8}$$

Equations of the form (8) were the basis of a mathematical model of electrical properties of a myelinated nerve which describes the time course of events following stimulus application and up to the initiation of the action potential. This model, described in [16], was validated by experiments.

By studying equation (8) J.Bell and C.Cosner [4] obtained sufficient conditions on the function f to guarantee that every node goes to the fully activated state. That is,

$$\lim_{t\to\infty} v_j(t) = 1, \qquad \forall j \in Z.$$

In particular, we must have $\int_0^1 f(t)dt > 0$, from where it follows that $a < 0.5$. Systems like (8) are often called lattice equations. They can be easily reduced to a mixed-type functional differential equation, if we assume that

$$v_{k+1}(t) = v_k(t - \tau),$$

where τ is a certain delay, more precisely, the time taken by an electrical signal to reach the neighbour node, which is proportional to the space between nodes and to the reciprocal of the propagation speed. By assuming this, we consider that the Ranvier nodes are uniformly distributed and that the electric pulse is propagating with a constant speed. Acording to [3], neurons in the central nervous system tend to have much more variability than those in the peripheral nervous system; therefore, when we assume that the nodes are identical electrically and uniformly distributed, the model is more appropriate for describing processes in the peripheral nervous system. Under these assumptions, in [5], Chi and his co-authors obtained the following equation

$$\frac{1}{R}(v(t-\tau) - 2v(t) + v(t+\tau)) + f(v(t)) = C\frac{dv(t)}{dt}, \tag{9}$$

where v represents the potential at a certain node (in this case, the potential at the neighbouring nodes is represented by $v(t-\tau)$ and $v(t+\tau)$). In the rest of this paper we will be concerned with equation (9), called the discrete FitzHugh-Nagumo equation.

During the last 20 years, equations of the type (9) have been the subject of research in many works, both theoretical and computational. In [15] and [23] important existence results were obtained. Computational approaches for the numerical solution of this and related problems have been presented by different authors, including Abell et al. [1], Elmer and Van Vleck [6], Hupkes and Verduyn-Lunel [12], Lima et al.[14].

We emphasize that the mathematical modelling of nerve conduction in myelinated axons is an active subject of research and very recently new approaches to this topic have appeared in the literature. We refer to a stochastic version of the FitzHugh-Nagumo equations (3), analysed in [10], and a new method for computing the characteristic length of myelinated segments in axons, described in [18].

The outline of this paper is as follows. In section 2, we set boundary conditions and analyse the asymptotic behaviour of solutions at infinity. In section 3, we discuss computational methods for numerical approximation. In section 4, we provide some numerical results and we finish with some conclusions in section 5.

2. The discrete FitzHugh-Nagumo equation

2.1. Statement of the boundary value problem

Let us rewrite equation (9) in the form

$$RCv'(t) = f(v(t)) + v(t-\tau) - 2v(t) + v(t+\tau). \tag{10}$$

4

As in [5], we introduce the new variables $t' = t/RC$, $\tau' = \tau/RC$, in order to obtain a nondimensionalised model. Moreover, for the sake of simplicity, we keep the previous notation for the variables, so that we consider the following equation:

$$v'(t) = f(v(t)) + v(t - \tau) - 2v(t) + v(t + \tau). \tag{11}$$

Due to the form of f, given by (7), equation (11) has two stable equilibrium points: $v = 0$ (resting potential) and $v = 1$ (fully activated potential). Therefore, we are interested in a solution of (11), increasing on $]-\infty, \infty[$, which satisfies the boundary conditions

$$\lim_{t \to -\infty} v(t) = 0, \qquad \lim_{t \to +\infty} v(t) = 1. \tag{12}$$

These conditions will be satisfied by the potential at any node. In order to guarantee uniqueness of solution, we add the condition

$$v(0) = 1/2. \tag{13}$$

We are interested in a **monotone** solution of problem (10)-(13), that is, we assume that once the signal starts propagating, the potential will increase at every node, tending to its maximal value ($v(t) = 1$). Such a solution exists for a certain value of τ, which must be computed.

2.2. Asymptotic approximation at infinity

Since in the next section we describe computational methods for the numerical solution of the given problem, it is desirable to study the asymptotic behaviour of the required solution at infinity, so that we can truncate the domain where this solution needs to be computed.

An extensive analysis of this behaviour has been provided in [5], so here we will just recall the main results from that paper.

Let us first consider the case where $t \to -\infty$. According to the conditions (12), $v(-\infty) = 0$, so that in order to linearise equation (10) about this point, we first use the Taylor expansion for the function f:

$$f(v) = f(0) + vf'(0) + \frac{v^2}{2}f''(0) + o(v^2) = vf'(0) + \frac{v^2}{2}f''(0) + o(v^2), \tag{14}$$

where f is given by (7).

As usual, in order to obtain a characteristic equation for (11) at $-\infty$ we replace f by the main term of its Taylor expansion and assume that v has the form

$$v_-(t) = \epsilon_- e^{\lambda(t+L)}, \tag{15}$$

where L is a sufficiently large parameter and ϵ_- is an estimate for $v_-(-L)$. In this way we obtain the equation

$$\lambda + 2 - f'(0) - 2\cosh(\lambda\tau) = 0. \tag{16}$$

This equation has two real roots; since we are interested in a function v_- that tends to 0 at $-\infty$, we choose the positive one, which we denote by λ_+.

The case where $t \to \infty$ can be handled in an analogous way. In this case, we have the following Taylor expansion for f:

$$f(v) = f(1) + (v - 1)f'(1) + \frac{(v-1)^2}{2}f''(1) + o((v-1)^2) \tag{17}$$

Moreover, as $t \to +\infty$, we assume that v has the form

$$v_+(t) = 1 - \epsilon_+ e^{\lambda(t-L)}, \tag{18}$$

5

where ϵ_+ is an estimate of $1 - v_+(L)$. In this way we obtain the characteristic equation

$$\lambda + 2 - f'(1) - 2\cosh(\lambda\tau) = 0 \tag{19}$$

In this case we choose the negative root of the characteristic equation, which we will denote by λ_-, in order to have $v_+(t) \to 1$, as $t \to +\infty$.

Now we have obtained two representations for the solution of our problem, (15) and (18), which we shall use to approximate the solution, for $t < -L$ and $t > L$, respectively, where L is a sufficiently large number. According to the form of equation (11), L must be a multiple of the delay τ; in our computations we have used $L = k\tau$, where $2 \le k \le 9$, depending on the specific problem (as discussed in Sec. 4).

These representations of the solution are used in the computational methods to replace the boundary conditions (12). In the next section we will show how this can be achieved.

3. Computational methods

In this section we will describe and compare some computational methods that can be applied to obtain approximate solutions of the problem (11), (12), (13). Since the problem is nonlinear, some of the considered methods require initial approximations, which must be sufficiently close to the true solution, to guarantee the convergence of the process. Thus we begin by presenting some preliminary results, which can help us to build a rough approximation of the solution.

3.1. Finding an initial approximation for the iterative process

The evaluation of τ (which represents both the unknown advance and delay in equation (11)) is a key point for the solution of the problem. As stated before, τ is one of the unknowns of the problem and physically is the reciprocal of the propagation speed. It is possible to approximate the value of τ in the problem by considering the parabolic equation

$$\frac{\partial u}{\partial t} = \frac{\partial^2 u}{\partial s^2} + bu(u - 1)(a - u), \tag{20}$$

which looks like the first equation of system (3). A function ϕ is said to be a travelling wave solution of (20) if for some solution u of (20) and some positive constant d we have

$$\phi(x + d\,t) = u(x, t), \qquad \forall x, t \in I\!R. \tag{21}$$

In this case d is called the propagation speed of the travelling wave. This problem was analysed, for example, in [2], [7], [19], [20]. In [2] and [7] the authors have studied the existence and stability of travelling waves which satisfy the conditions $\phi(-\infty) = 0$, $\phi(\infty) = 1$, for a class of diffusion equations, which includes (20) as a particular case. By substituting (21) into the original partial differential equation a singular boundary value problem is obtained for a second order ordinary differential equation of the form:

$$u''(x) - gu(x) + n(x)f(u) = 0,$$

where g and and n are a constant and a given function, respectively. Equations of this form were analysed, for example, in [22].

As shown in [2] and [7], the boundary value problem is solvable only for a certain value of d. In the particular case of (20), assuming that $a < 1/2$, this value can be determined analytically (see [13]):

$$d = \frac{(1 - 2a)\sqrt{b}}{\sqrt{2}}. \tag{22}$$

6

Since τ, as we have said, is proportional to the reciprocal of the propagation speed, from (22) we can obtain the following estimate of τ:

$$\tau \approx \tau_0 = \frac{1}{d} = \frac{\sqrt{2}}{(1-2a)\sqrt{b}}. \tag{23}$$

Once τ_0 is computed from (23), approximate values of the characteristic roots λ_+ and λ_- can be computed from (16) and (19), respectively.

An approximate solution of the problem (11),(12), (13) can then be found in the form:

$$v_0(t) = \begin{cases} C_1 e^{\lambda_+ t}, & for \quad t < 0, \\ 1 - C_2 e^{\lambda_- t}, & for \quad t \geq 0, \end{cases} \tag{24}$$

where the constants C_1 and C_2 can be determined from the condition that

$$\lim_{t \to 0-} v_0(t) = \lim_{t \to 0+} v_0(t) = \frac{1}{2}.$$

Some numerical results illustrating this approximation will be presented in section 4.

We shall now describe an alternative approach to obtain an estimate of τ and an approximate solution, which does not require the use of the formula (22). Taking into account the conditions (12) and (13) and the asymptotic behaviour of v for large values of t, described by (15) and (18), we search for an approximate solution of the considered problem in the form

$$v_1(t) = \frac{1}{2}(1 + \tanh(ct)), \tag{25}$$

where $c \in \mathbb{R}^+$. In order to evaluate c we use the condition that v_1 satisfies equation (11) at $t = 0$. More precisely, we write:

$$v_1'(0) = v_1(\tau) + v_1(-\tau) - 2v_1(0) + f(v_1(0)) \tag{26}$$

Taking into account that tanh is an odd function, from (25) and (26) it follows that

$$v_1'(0) = f(v_1(0)) = f(1/2). \tag{27}$$

On the other hand, we have

$$v_1'(0) = \frac{c}{2} \tag{28}$$

From (27) and (28) we finally conclude that

$$c = 2f(\frac{1}{2}). \tag{29}$$

Now we can use the approximate solution v_1 to obtain estimates of λ_+ and τ. We can easily observe that

$$v_1(t) = \frac{1}{2}\left(1 + \frac{e^{2ct} - 1}{e^{2ct} + 1}\right) = e^{2ct} + O(e^{4ct}), \qquad as\, t \to -\infty. \tag{30}$$

Taking into account the asymptotic behaviour of v as $t \to -\infty$, given by (15), we obtain the following approximation for λ_+:

$$\lambda_+ \approx 2c = 4f(\frac{1}{2}). \tag{31}$$

7

Finally, having an approximate value for λ_+, we can evaluate τ from (16), which gives us the estimate

$$\tau_1 = \frac{1}{\lambda_+} arccosh \left(\frac{\lambda_+ + 2 - f'(0)}{2} \right). \tag{32}$$

By similar arguments, we can obtain the following approximation for λ_-:

$$\lambda_- \approx -2c = -4f(\frac{1}{2}). \tag{33}$$

Using (33) and (19) we can also obtain an estimate for τ.

Finally we present a more sophisticated estimate, which results from approximating the solution by a piecewise differentiable function. We search for an approximate solution of the considered problem in the form

$$v_2(t) = \begin{cases} \epsilon_- e^{\lambda_+ (t+2\tau)}, & if \quad t < -2\tau; \\ a_0 + a_1 t + a_2 t^2, & if \quad -2\tau \le t < -\tau; \\ \frac{1}{2} + b_1 t + b_2 t^2 + b_3 t^3, & if \quad -\tau \le t < 0; \\ \frac{1}{2} + c_1 t + c_2 t^2 + c_3 t^3 & if \quad 0 < t < \tau; \\ d_0 + d_1 t + d_2 t^2, & if \quad \tau \le t < 2\tau; \\ 1 - \epsilon_+ e^{\lambda_- (t-2\tau)}, & if \quad t \ge 2\tau; \end{cases} \tag{34}$$

From the form of v_2 if follows that this function satisfies the boundary conditions (12) and (13). We easily see that v_2 depends on 17 parameters: $\tau, \epsilon_-, \epsilon_+, \lambda_-, \lambda_+, a_0, a_1, a_2, b_1, b_2, b_3, c_1, c_2, c_3, d_0, d_1, d_2$. These coefficients are computed from a system of 17 equations, which include

- the two characteristic equations (16) and (19);

- two equations that assure the continuity of v_2 and v_2' at -2τ;

- two equations that assure the continuity of v_2 and v_2' at $-\tau$;

- two equations that assures the continuity of v_2' and v_2'' at 0;

- two equations that assure the continuity of v_2 and v_2' at τ;

- two equations that assure the continuity of v_2 and v_2' at 2τ;

- five equations that assure that v_2 satisfies (11) at $t = -2\tau, t = -\tau, t = 0, t = \tau$ and $t = 2\tau$.

The nonlinear system of equations can be solved by the Newton method. The stimates for λ_-, λ_+ and τ from above can be used as initial approximations. As follows easily from the construction, $v_2 \in C^1(I\!R)$. Some examples of application of this approximation will also be given in section 4.

Though it is not possible to prove theoretically the convergence of the Newton method applied to this system, there is numerical evidence showing that it converges when a and b are within the ranges considered in this work. Moreover, analytical arguments support this evidence. In particular, all the equations of this system are given by continuously differentiable functions, so that the system has a continuous Jacobian matrix. We cannot prove a priori that this matrix is invertible in all the cases of interest, but we have used Mathematica software [21], which warns the user whenever it is close to a singular matrix. Moreover, the fact that we use as initial approximations for $\lambda_-, \lambda-+, \tau$ values that we have obtained from (31),(32),(33) explains the success of the Newton method. Finally, we emphasise that all the numerical results obtained from the solution of this nonlinear system (which will be discussed in Sec. 4), have the correct qualitative behaviour and are in agreement with the results obtained by other methods.

3.2. A method of steps approach

In this section we describe an approach, based on the method of steps, to find a solution to the problem considered by Chi, Bell and Hassard in [5] and outlined in section 2 of this paper. For the convenience of the reader we repeat the four relevant equations here.

$$\lambda_+ + 2 - f'(0) - 2\cosh(\lambda_+\tau) = 0 \tag{35}$$

$$\lambda_- + 2 - f'(1) - 2\cosh(\lambda_-\tau) = 0 \tag{36}$$

$$v_-(0) = 0.5 \tag{37}$$

$$v_+(0) = 0.5 \tag{38}$$

Following the approach in [5] we use the approximations $v_-(t) = \epsilon_- e^{\lambda_+(t+L)}$ for $t < -L$ and $v_+(t) = 1 - \epsilon_+ e^{\lambda_-(t-L)}$ for $t > L$. We set $L = m\tau, m \in \mathbf{N}$. We observe that for a specified value of τ equations (35) and (36) can be solved using the Newton-Raphson method to find λ_+ and λ_- respectively. With λ_+ and λ_- known, each of equations (37) and (38) involve only one unknown parameter, and a bisection method can be used to find the associated values of ϵ_- and ϵ_+.

Given that values of $\lambda_+, \lambda_-, \epsilon_+$ and ϵ_- can be found for a specified value of τ the problem then becomes one of choosing the appropriate value of τ. We require that the solution be *smooth* at the origin. Following experimentation with the aim of finding τ such that $v'_-(0) = v'_+(0)$, and encountering problems with numerical instability affecting the gradient, we have adopted the following method to establish τ. We use equation (11) with $f(v) = bv(1-v)(v-a)$, a central difference approximation for $v'(t)$ and a step length $h = \frac{\tau}{N}$, and write

$$\frac{1}{2h}(v_{n+1} - v_{n-1}) = bv_n(1-v_n)(v_n - a) + v_{n-N} - 2v_n + v_{n+N}. \tag{39}$$

We can rearrange (39) to give

$$v_{n+N} = \frac{1}{2h}(v_{n+1} - v_{n-1}) - bv_n(1-v_n)(v_n - a) - v_{n-N} + 2v_n, \tag{40}$$

which, when we let $i = n + N$, leads to

$$v_i = \frac{1}{2h}(v_{i-N+1} - v_{i-N-1}) - bv_{i-N}(1-v_{i-N})(v_{i-N} - a) - v_{i-2N} + 2v_{i-N}. \tag{41}$$

Using (41) for $t \geq -L$, and $v_-(t) = \epsilon_- e^{\lambda_+(t+l)}$ for $t < -L$, we can compute a solution for $t \geq -L$. In a similar way we can derive

$$v_j = \frac{1}{2h}(v_{j+N+1} - v_{j+N-1}) - bv_{j+N}(1-v_{j+N})(v_{j+N} - a) - v_{j+2N} + 2v_{j+N}$$

and use this, along with $v_+(t) = 1 - \epsilon_+ e^{\lambda_-(t-L)}$ for $t > L$, to compute a solution for $t \leq L$. We have thus found a solution *forwards* for $t \geq -L$ and a solution *backwards* for $t \leq L$. Ideally these solutions would be identical in order to be consistent with the equation in use. To obtain as smooth a solution as possible near to the origin we find forwards and backwards solution vectors, F_1 and F_2, on an interval of the form $[-k\tau, k\tau]$ and choose τ to minimise $\frac{(F_2-F_1).(F_2-F_1)}{2kN+1}$, that is, we find τ to minimise the average squared 'distance' between the two solutions at the grid points. The solution curve can then be plotted using the calculated parameter values. The numerical resultes obtained by this method will be presented and discussed in Sec. 4.2.

3.3. Finite difference method

In this section we describe a finite difference scheme for the solution of problem (11), (12), (13). This scheme has some common features with the one described in [5], but it has the advantage that it can be easily solved by the Newton iterative method, without using the continuation algorithm. As an initial approximation for the Newton method we have used the function v_2, defined by (34).

In order to approximate the solution we introduce on $[-K\tau, K\tau]$ a uniform mesh with stepsize $h = \tau/N$. Let $t_i = -K\tau + ih$, $i = 0, ..., 2KN$ be the nodes of this mesh. Here K is a sufficiently large integer so that $\epsilon_1 = v(-K\tau)$ is comparable with h^2 (the reason for this choice will be explained below). As in [5], the first derivative is approximated by a 4-th order finite difference:

$$v'(t_i) \approx L_h(v)_i = \frac{1}{h}\left(\frac{2}{3}(v(t_{i+1}) - v(t_{i-1})) - \frac{1}{12}(v(t_{i+2}) - v(t_{i-2}))\right). \tag{42}$$

By using this approximation at each node t_i we obtain $2KN + 1$ equations of the form:

$$L_h(v)_i = v(t_i + \tau) + v(t_i - \tau) - 2v(t_i) + f(v(t_i)) + r_i^h, \tag{43}$$

where $\|r_h^i\| = O(h^4)$. Note that for $t_i > (K-1)\tau$ and $t_i < -(K-1)\tau$ equation (43) involves the value of v at one or more points that do not belong to the interval $[-K\tau, K\tau]$. In this case the boundary conditions (12) are applied, by considering the fact that v satisfies (15) or (18), when $v < -K\tau$ or $v > K\tau$, respectively. In this way, we write

$$v(-K\tau - x) = v(-K\tau)e^{-\lambda_+ x}, \qquad (x > 0), \tag{44}$$

$$1 - v(K\tau + x) = (1 - v(K\tau))e^{-\lambda_- x}, \qquad (x > 0). \tag{45}$$

Finally, by ignoring r_i^h in (43), we obtain $(2K - 2)N$ finite difference equations of the form:

$$L_h(v)_i = v_{i+N} + v_{i-N} - 2v_i + f(v_i), \qquad i = N + 1, ..., (2K - 1)N + 1. \tag{46}$$

Here as usual v_i represents the approximate value of $v(t_i)$. For $0 \le i < N+1$ and $(2K-1)N+1 < i \le 2KN+1$, we have modifications of equation (46) which result from applying formulae (44) or (45), respectively. This gives a system of $2KN + 1$ equations, which is then completed with the equation $v_{KN} = 1/2$, resulting from (13). Moreover, we have the characteristic equations (16) and (19), making a total of $2KN + 4$ equations. Note that the number of unknowns is also $2KN + 4$: $2KN + 1$ entries of the vector $v = (v_0, ..., v_{2KN})$, λ_-, λ_+ and τ.

This nonlinear system is then solved by the Newton method. The Jacobian matrix for the Newton method has at most 8 nonzero entries at each row: 7 corresponding to the unknowns v_{i-N}, v_{i-2}, v_{i-1}, v_i, v_{i+1}, v_{i+2}, v_{i+N}; one corresponding to τ.

Although the condition number of the Jacobian matrices increases with the the number of gridpoints in the scheme (as could be expected), it is remarkable that even for the finest meshes it doesn't become very large. Even in the case of $n = 2^8$ and $K = 9$, the condition numbers do not get higher than 10^5. As we shall see below, this enables us to obtain accurate results, within a large range of values of a and b.

It is well known that the Newton method is very sensitive to the choice of initial approximation, especially in the case of large dimensional systems. In our case, as stated above, we have overcome this problem by using as initial approximation to v the function v_2, described in the previous section, and the corresponding approximations to λ_-, λ_+ and τ.

a	τ_0	τ_1	τ_2	τ_3	τ	λ_-	λ_+
0	0.3651	0.2987	0.3101	0.38186	0.38029	-6.22752	5.1007
0.05	0.4057	0.3318	0.3461	0.43482	0.43511	-5.44866	4.5111
0.1	0.4564	0.3734	0.3910	0.50376	0.5056	-4.6909	3.9297
0.15	0.5216	0.4267	0.4485	0.59156	0.5993	-3.95523	3.3586
0.2	0.6086	0.4978	0.5250	0.69607	0.73001	-3.32594	2.6073
0.25	0.7303	0.5973	0.6318	0.83500	0.92525	-2.55197	2.2691
0.3	0.9129	0.7467	0.7916	0.97366	1.2515	-1.88069	1.66568
0.35	1.2172	0.9956	1.0575	0.97515	1.9371	-1.2111	1.08772

Table 1: Estimates of τ, λ_- and λ_+ for different values of a, with $b = 15$

.

b	τ_0	τ_1	τ_2	τ_3	τ	λ_-	λ_+
1	1.571	1.540	1.652	0.9835	1.6250	-0.4333	0.4096
5	0.7027	0.6447	0.6639	0.7517	0.7229	-2.0677	1.8678
11	0.4738	0.4034	0.4325	0.5087	0.5008	-4.1869	3.5574
16	0.3928	0.3184	0.3296	0.4231	0.4227	-5.7499	4.7354
21	0.3429	0.2666	0.2656	0.3678	0.3744	-7.1795	5.7840
51	0.2200	0.1443	0.1216	0.1200	0.2554	-14.0692	10.6338

Table 2: Estimates of τ, λ_- and λ_+ for different values of b, with $a = 0.05$

.

4. Numerical results

4.1. Comparison of initial approximations

In this subsection we compare the estimates of τ and v obtained by the different methods described in Sec. 3.1. In all the cases we consider the problem (11), (12), (13). We denote by τ_0 the estimate obtained by (23); τ_1 is the estimate obtained by (32) and τ_2 is the one obtained when using the approximating function v_2, defined by (34); τ stands for the value obtained by the finite difference method with $N = 64$, which is the most accurate approximation (see detailed analysis in the next subsection). Table 1 contains the estimates of τ, for $b = 15$, with different values of a. The values of τ obtained in the case $a = 0.05$, for different values of b, are displayed in Table 2.

In the same tables we also give for comparison the estimates of τ (denoted as τ_3) obtained by the method of steps, described in Sec 3.2. For a more detailed discussion of these results see the next subsection. The errors of τ_0, τ_1, τ_2 and τ_3 can be obtained by comparing these estimates with τ, which can be considered as the exact value for this purpose. Notice that the presented values of τ coincide with those obtained in [5], within the given precision.

The approximate values of λ_- and λ_+ obtained by the finite difference method, with $N = 64$, are given in the two last columns of the mentioned tables.

The comparison of the listed estimates leads us to the conclusion that, for $0 \le a \le 0.3$ and $5 \le b \le 21$

$$|\tau_3 - \tau| < |\tau_0 - \tau| < |\tau_2 - \tau| < |\tau_1 - \tau|,$$

that is, for this range of values of a and b the most accurate approximation among those studied in Sec. 3.1 and Sec. 3.2. is τ_3 and the least acurate is τ_1. All the estimates preserve the main characteristics of

11

b	$v_1'(0)$	$v_2'(0)$	$v_3'(0)$	$v'(0)$
1	0.1125	0.1224	–	0.112695
5	0.5625	0.6045	0.59429	0.58339
11	1.2375	1.2821	1.2795	1.2774
16	1.8000	1.83603	1.83803	1.84116
21	2.3625	2.39174	2.39578	2.40116
51	5.7375	5.7504	4.33730	5.76174

Table 3: Estimates of $v'(0)$ for different values of b, with $a = 0.05$

.

a	$v_1'(0)$	$v_2'(0)$	$v_3'(0)$	$v'(0)$
0	1.875	1.9171	1.9019	1.9181
0.05	1.6875	1.72515	1.71512	1.72889
0.1	1.5000	1.53326	1.52735	1.53918
0.15	1.3125	1.34141	1.33830	1.34891
0.2	1.125	1.1496	1.14711	1.1580
0.25	0.9375	0.957907	0.955325	0.96647
0.3	0.7500	0.76624	0.760515	0.774237
0.35	0.5625	0.57463	0.55987	0.58131

Table 4: Estimates of $v'(0)$ for different values of a, with $b = 15$.

τ, as a function of a and b: they increase with a and decrease, as b increases.This behaviour agrees with the physical meaning of the variables. Since a is the threshold potential, the propagation speed is supposed to decrease as a increases, and therefore we observe τ increasing. On the other hand, increasing b means a higher potential at the nodes and this leads to a greater propagation speed and the decreasing of τ.

It is worth remarking that for values of a, greater then 0.3 large discrepancies between the different estimates arise. This is connected with the numerical instability of the different methods which is observed for the values of a we considered. In particular, in the case $a \geq 0.3$, the value τ obtained by the finite difference method seems to have a larger error than the other approximations (and this does not arise elsewhere). The explanation for this may be the instability which is also visible in the graphs of Figure 8. Note that according to the theoretical results, described in Sec.2, existence of a solution can be proved only for $a < 0.5$. The accuracy of the results is also reduced for values of b, greater than 21.

According to Keener [13], the discrete Nagumo equation has a "propagation failure" for sufficiently small coupling coefficient. When the equation is written in the form (11), a small coupling corresponds to high values of b. Thus when b is large the problem (11),(12),(13) becomes unsolvable. This explains why for high values of b estimates obtained by different methods differ significantly.

In Tables 3 and 4 numerical approximations for $v'(0)$, obtained by diferent methods, are given for a set of values of a and b. In agreement with the notation used in Tables 1 and 2, we denote by $v_i'(0)$ the estimate obtained by the method, corresponding to τ_i, $i = 1, 2, 3$. The approximations obtained by the finite difference method, with $N = 64$, are denoted simply by $v'(0)$. In this case the differences between the estimates obtained by different methods are not so large as in the case of the evaluation of τ. Even for $a > 0.3$ or $b > 21$, these differences are not greater than 5 per cent. This suggests that the gradient of the solution at the origin is not so sensitive to computational errors as the value of τ.

The graphs of v_0, v_1 and v_2 are plotted in fig.2, for $a = 0.3$ and $b = 15$.
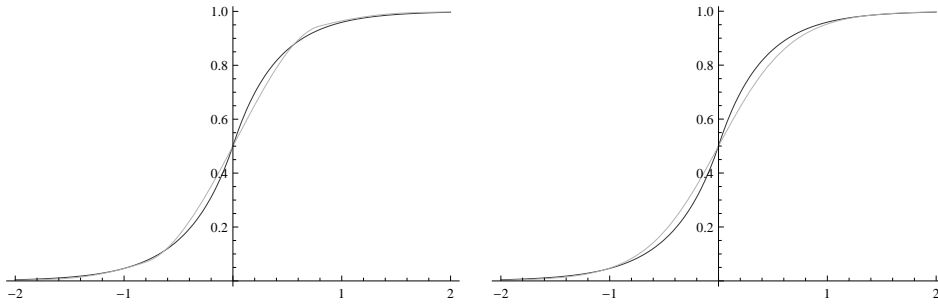
12

Figure 2: Graphs of v_0 (gray), v_2 (left side,black) and v_1 (right side, black).
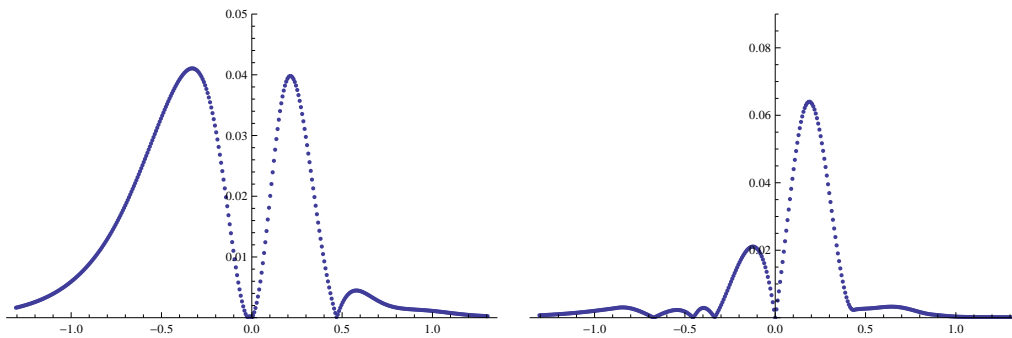

Figure 3: Absolute error of v_1 (left side) and v_2 (right side), with respect to the finite difference approximation.

In Figures 3 and 4 the absolute errors of the approximate solutions v_1, v_2 and v_0 are plotted (respectively), in the case $a = 0.05$, $b = 15$. By absolute error of v_i, we mean the difference $|v_i - v_h|$, where v_h is the finite difference approximation of the solution, obtained with $N = 256$. Note that, for all the approximations, the largest errors occur close to $t = 0$, where the solution changes faster. In this region the error can reach about 10 per cent of the solution value.

We remark that by differentiating v_1 and v_2 we obtain reasonable approximations of v'. In the case of v_0, the derivative is not continuous at $t = 0$ and the approximation is therefore much worse. The derivatives of v_1 and v_2 are plotted in fig.5. In both cases, the approximation of the derivative, obtained by the finite diference method, is also given, for comparison.

4.2. Numerical results by the method of steps

In this subsection we present results obtained by the method of steps, described in Sec. 3.2. Some of these results were also included in Tables 1 and 2, presented in Sec. 4.1.

To illustrate the application of this approach, and to provide some justification for the values of k and N used, we present some results arising from solving the problem with $m = 3$, $a = 0.05$ and $b = 15$ with several different step lengths and different values of k. In Table 5 we give estimated values of τ for $k = 0.5$, 1, 2 and 3 and include the mean square distance (shown in italics) between the two solution vectors F_1 and F_2) defined as in Section 3.2) We observe greater numerical instability for larger intervals (or larger values of k) and for smaller step lengths (or larger values of N). Although smaller mean squared differences (msd) are observed for smaller intervals, as can be seen from the equation, the derivative at $t = 0$ depends on the solution values at $-\tau$ and $+\tau$. To take these two values into account the solution vectors for $k = 1$ (that is,
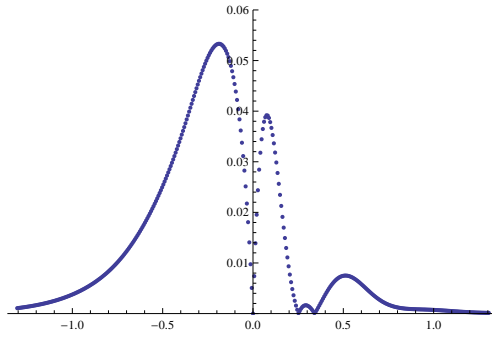
13

Figure 4: Absolute error of v_0, with respect to the finite difference approximation.
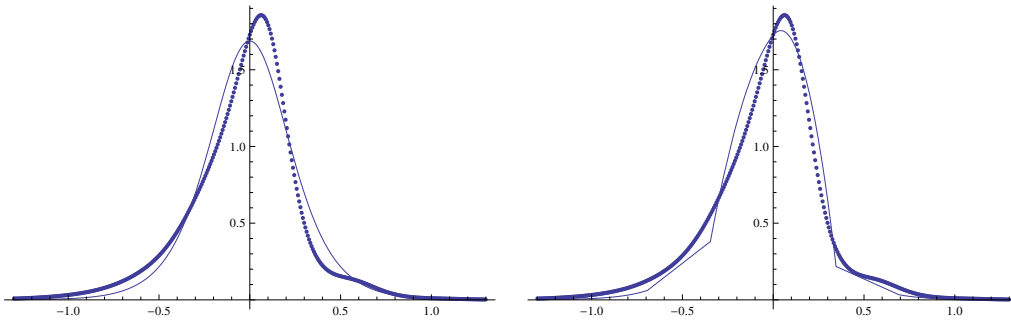

Figure 5: Approximations of the solution derivative: by the finite difference method (dotted line); using v_1 (continuous line, left side); and using v_2 (continuous line, right side).

14

a solution vector on an interval of length 2τ) have been used in the derivation of τ_3 in Tables 1 and 2. In Table 1 we use $N = 32$ and in Table 2 we use $N = 8$.

N	Length of interval for solution vectors F_1 and F_2				
	6τ (k=3)	4τ (k=2)	2τ (k=1)	τ (k=0.5)	0.5τ (k=0.25)
4	0.43350	0.43959	0.45625	0.43179	0.45567
	$2.0522{\times}10^5$	2.5647	$5.0617{\times}10^{-2}$	$7.3949{\times}10^{-3}$	$1.0284{\times}10^{-2}$
8	0.54313	0.46286	0.43693	0.41537	0.36073
	$3.0469{\times}10^6$	6.9371	$5.4510{\times}10^{-2}$	$1.6380{\times}10^{-2}$	$1.8850{\times}10^{-3}$
16	0.52188	0.50615	0.46576	0.41254	0.41770
	$1.8547{\times}10^7$	9.1956	$9.1752{\times}10^{-2}$	$1.6982{\times}10^{-2}$	$4.1313{\times}10^{-3}$
32	0.44313	0.44136	0.43482	0.42594	0.42745
	$6.6563{\times}10^{13}$	$8.9280{\times}10^2$	$2.5809{\times}10^{-1}$	$1.4856{\times}10^{-2}$	$2.6730{\times}10^{-3}$
64	0.43118	0.43596	0.45791	0.41636	0.41649
	$4.2084{\times}10^{30}$	$1.6415{\times}10^8$	$1.2501{\times}10^1$	$2.1327{\times}10^{-2}$	$1.1144{\times}10^{-2}$

Table 5: Estimates for τ and the mean square difference (*in italics*) as k and N vary. $[m = 3, a = 0.05, b = 15, h = \frac{\tau}{N}]$

A graphical representation of the *tools* used in the method is given in fig.6. Here we have used the values $m = 3, a = 0.1$ and $b = 15$. Diagram (a) illustrates the minimisation process used to find the *best* value of τ. Diagram (b) illustrates the *forwards* and *backwards* solutions, indicated by +++ and *** respectively, and gives a clear indication of why larger intervals for the solution vectors are inappropriate. Diagram (c) shows the two solution vectors for the value of τ selected by the method and diagram (d) shows the corresponding solution. Diagrams (e) and (f) have been included to illustrate the solution vectors and solution for an *incorrect* value of τ. We observe the larger variation in the msd and the lack of smoothness in the solution near the origin.

4.3. Numerical results for a test problem

With the purpose of testing the convergence and accuracy of the proposed numerical schemes it is useful to apply them to a test problem, whose exact solution is known. Such a problem is described in [5]. The function f on the right-hand side of (11) is replaced by

$$f_\theta(v) = \frac{1 + 2\theta(2v - 1) - (1 + \theta)(2v - 1)^2 - \theta(3 - 2v)(2v - 1)^3}{2(1 - \theta(2v - 1)^2)}, \tag{47}$$

where $\theta > 0$. In this case the exact solution is

$$v(t) = \frac{1 + \tanh(t)}{2}, \quad \tau = \tanh^{-1}(\sqrt{\theta}). \tag{48}$$

We have focused our attention on two test cases: $\theta = 0.35$ and $\theta = 0.7$; the corresponding values of τ can be obtained by (48): $\tau = 0.6801362704$ and $\tau = 1.209935121$, respectively. Numerical results for the first of these cases are also presented in [5].

By applying our numerical algorithm to this problem our main purposes are: 1) to test its accuracy and stability; 2) to observe how the error depends on the stepsize h and on the interval length L; 3) to choose optimal values for these parameters, in order to minimise the error.

15

Figure 6: A graphical illustration of the method of steps approach:$[m = 3, a = 0.1, b = 15, h = \frac{1}{32}]$

h	$e_h(K=3)$	$e_h(K=6)$	$e_h(K=9)$
$\tau/2^3$	$7.3E-4$	$2.60E-6$	$2.47E-6$
$\tau/2^4$	$7.9E-4$	$2.89E-7$	$1.55E-7$
$\tau/2^5$	$8.3E-4$	$1.48E-7$	$9.72E-9$
$\tau/2^6$	$8.5E-4$	$1.42E-7$	$6.35E-10$
$\tau/2^7$	$8.6E-4$	$1.42E-7$	$6.76E-11$
$\tau/2^8$	$8.6E-4$	$1.43E-7$	$3.22E-11$
ϵ	0.017	$2.96E-4$	$5.29E-6$

Table 6: Errors in the approximation of τ, in the case of the test problem with $\theta = 0.35$, for different values of h and K

Concerning h, since we are using a sheme of 4-th order approximation, we expect an error of the order $O(h^4)$. In order to keep the dimension of the matrices in the finite difference scheme not too high, we have chosen to use stepsizes not smaller than $h_{min} = \tau/2^8$. In this case we have in most examples $10^{-12} < h_{min}^4 < 10^{-11}$.

The choice of the interval length L is based on the values of $\epsilon_1 = v(-L)$ and $\epsilon_2 = 1 - v(L)$ (see (15),(18)). We recall that when replacing f by its Taylor expansion as $v \approx 0$ and $v \approx 1$ (see (14) and (17)) we introduce errors of the order ϵ_1^2 and ϵ_2^2, respectively. Therefore, it makes sense to choose L such that ϵ^2 has the same order as h_{min}^4, where $\epsilon = \max(\epsilon_1, \epsilon_2)$. In this way the error introduced by the truncation of the real line has approximately the same order as the discretisation error. Since in our finite difference scheme we have $L = K\tau$, the choice of the integer K determines the value of L. Thus we must choose K large enough to obtain $\epsilon \approx h_{min}^2$. Of course ϵ depends not only on the length L but also on the decay rate of the solution, so the optimal value of K (and L) may differ substantially from one problem to another.

This can be seen in Tables 6 and 7, which contain the errors $e_h = \tau_h - \tau$, where τ_h denotes the approximate value obtained with stepsize h. In each table, the errors are given for different values of h and K; the value of ϵ is also given for each K. Table 6 contains the results for the case $\theta = 0.35$. In this case it is clear that when using $K = 3$ ($L = 3\tau \approx 2.04$) the approximation error is never less than 0.00073, no matter how much the stepsize is reduced. By increasing the value of K to 6 it is possible to improve the accuracy: using the stepsize $h = \tau/2^6$ the error reduces to 1.42×10^{-7}. This accuracy can be improved further by using $K = 9$; in this case the error becomes as small as 3.22×10^{-11} (with stepsize $h = \tau/2^8$). This is nearly the optimal value of K (for the given minimal stepsize), since further increasing K doesn't change the results significantly. In this way we confirm the above criterion for the choice of L: we must choose L such that $\epsilon \approx h_{min}^2$ (see the values of ϵ in the same table).

The corresponding values for the case $\theta = 0.7$ are displayed in Table 7. In this case it can be seen that the optimal value of K is 6 (by choosing $K = 9$ no significant change is obtained in the results). This again confirms the criterion for the choice of L.

4.4. Numerical results for the target problem

In this subsection we present numerical results for the problem (11)-(13), obtained by the method described in Sec.3.3. We have tested numerically the convergence order of the method. When the exact solution is not known, an estimate of the convergence order can be obtained from three finite difference solutions, obtained with different stepsizes: $v_{2h}, v_h, v_{h/2}$, where $h > 0$. The estimate of the convergence order is then given by

$$p = \log_2 \frac{\|v_h - v_{2h}\|}{\|v_h - v_{h/2}\|},$$

17

h	$e_h(K=3)$	$e_h(K=6)$
$\tau/2^3$	$9.53E-6$	$9.34E-6$
$\tau/2^4$	$8.30E-7$	$6.05E-7$
$\tau/2^5$	$2.92E-7$	$3.81E-8$
$\tau/2^6$	$2.71E-7$	$2.39E-9$
$\tau/2^7$	$2.76E-7$	$1.49E-10$
$\tau/2^8$	$2.79E-7$	$9.33E-12$
ϵ	$7.3E-4$	$4.95E-7$

Table 7: Errors in the approximation of τ, in the case of the test problem with $\theta = 0.7$, for different values of h and K

h	$\|v_h - v_{2h}\|$	p
$\tau/2^4$	$1.51E-5$	6.22
$\tau/2^5$	$2.03E-7$	3.981
$\tau/2^6$	$1.29E-8$	3.994
$\tau/2^7$	$0.07E-10$	3.998
$\tau/2^8$	$5.05E-11$	

Table 8: Estimates of convergence order in the case $a = 0.05, b = 5$, with $K = 9$.

where the maximum norm is used. The numerical results displayed in Tables 8, 9, 10 suggest that the method has 4-th order convergence, as could be expected. The value of K, which determines the interval length, was chosen in each example using the criterion described in the previous section, based on the value of ϵ. In order to illustrate the application of this criterion, in Table 11 we display the values of ϵ, for the three considered examples, with different values of K. Note, that when the chosen value of K is not large enough, there is a drop in the estimated convergence order, which is due to the error resulting from the truncation of the interval. On the other hand, the use of too large a value of K makes the method less efficient, requiring the use of large matrices, without improving the accuracy.

The large differences between the estimates of τ, obtained by various methods, observed in Sec. 4.1, for certain values of a and b suggest that some of the computational methods may become unstable for such values, in particular, when a is close to 0.5 or b is large. This is true, in particular, in the case of the finite difference method, as is shown by the graphs of the approximate solutions plotted in fig.7 and fig.8.

As mentioned in subsection 3.3, the finite difference method developed in this work was inspired by the method described in [5] . However, the algorithm described in that work relies on the continuation method, that is, a numerical solution is first computed for a test problem and then, by a continuous change of a parameter, a sequence of auxiliary equations is solved, until reaching the target problem. Possibly following

h	$\|v_h - v_{2h}\|$	p
$\tau/2^4$	0.015	7.42
$\tau/2^5$	$8.80E-5$	5.11
$\tau/2^6$	$2.55E-6$	3.97
$\tau/2^7$	$1.63E-7$	3.99
$\tau/2^8$	$1.02E-8$	

Table 9: Estimates of convergence order in the case $a = 0.05, b = 15$, with $K = 6$.

h	$\|v_h - v_{2h}\|$	p
$\tau/2^4$	0.00041	6.518
$\tau/2^5$	$4.48E-6$	3.973
$\tau/2^6$	$2.85E-7$	3.992
$\tau/2^7$	$1.79E-8$	3.998
$\tau/2^8$	$1.12E-9$	

Table 10: Estimates of convergence order in the case $a = 0.05, b = 21$, with $K = 6$

K	$b = 5$	$b = 15$	$b = 21$
3	$1.29E-2$	$1.80E-3$	$2.50E-3$
6	$2.30E-4$	$\mathbf{4.98E-6}$	$\mathbf{1.91E-6}$
9	$\mathbf{3.96E-6}$	$1.37E-8$	$2.63E-9$

Table 11: Values of ϵ, for different K, in the three examples considered above. The value corresponding to the chosen K is written in boldface.

on from this, the results reported in [5] are limited to the cases where $a \leq 0.2$ and $b \leq 20$. In our numerical experiments, the initial approximations for the Newton method were obtained by the numerical methods described in subsection 3.1; this enabled us to solve the problem for a wider range of values of a and b. Moreover, our algorithm worked with stepsizes as small as 0.001, while in the case of the numerical results reported in [5] the typical stepsize was $h = 0.05$.

5. Conclusions

We have applied several computational approaches to the solution of the problem (11)-(12), analysed and compared the numerical results. The most accurate results are obtained by the finite difference method, described in Sec. 3.3. The convergence of this method was tested in a model problem, whose exact solution is known, and its performance is very good, showing 4-th order convergence and giving results with up to 11 exact digits, within a reasonable computational effort.

This is also true for the case of the target problem, when the problem parameters satisfy $0 \leq a < 0.3$ and $5 \leq b \leq 51$. However, for other values of the parameters computational instability arises.
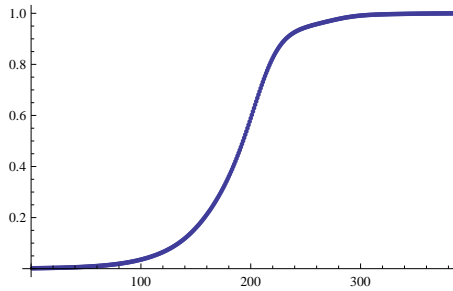

Figure 7: Graph of the numerical solution obtained by the finite difference method with $N = 64$, in the case $a = 0.1, b = 15$. Here the numerical solution preserves the smoothness of the true solution.
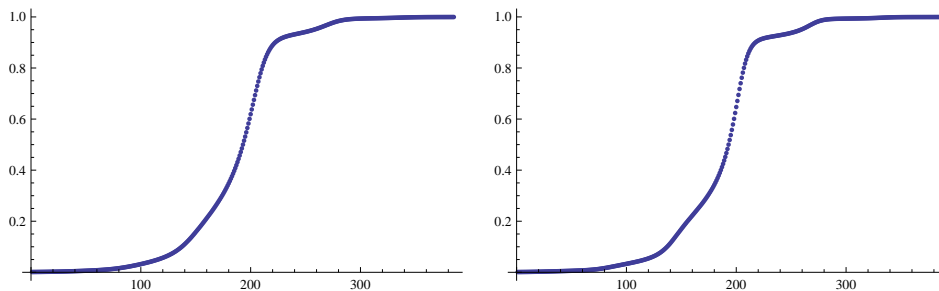
Figure 8: Graphs of numerical solutions obtained by the finite difference method with $N = 64$, in the cases $a = 0.3, b = 15$ (left side), $a = 0.35, b = 15$ (right side). Here the effect of numerical instability is evident.

The approach based on the method of steps, described in Sec. 3.2, gives a good approximation but its accuracy is limited by the fact that the discretisation step cannot be very small (for $N > 32$ numerical instability arises). The estimates of τ obtained by this method have a relative error of about 1 per cent.

Three other approximation methods were discussed in Sec. 3.1 . The computational effort required by these methods is very small and the algorithms are very simple. Although their accuracy is reduced, they can provide good initial approximations for the finite difference method.

The numerical results obtained in our paper confirm the main features of the considered mathematical model. In particular, it was observed that the propagation speed $(1/\tau)$ increases as the threshold potential a decreases (see table 1) and as the intensity of the ionic currents (represented by b) increases (see table 2). The typical S-shaped form of the solution graphic (illustrated by fig. 7, for example) means that the potential changes slowly when it is close to its resting or fully activated value; and changes fast, when it is close to the average value. As a consequence, the solution derivative takes its highest values when t is close to 0, and these values are particularly high when a is small and b is large (as it follows from tables 3 and 4). Finally, the fact that the method fails to produce an acceptable solution approximation for $a > 0.3$ is not surprising, since it is known that propagation failures may occur for high values of a.

Acknowledgement

References

[1] K. A. Abell, C.E. Elmer, A.R. Humphries, E.S. Vleck, Computation of mixed type functional differential boundary value problems, SIAM J. Appl. Dyn. Syst., 4 (2005), 755–781.

[2] D.G. Aronson and H.F. Weinberger, Nonlinear diffusion in population genetics, combustion and nerve propagation, in Lecture Notes in Mathematics, 444, Springer, Berlin, New York, 1975, 5–49.

[3] J. Bell, Behaviour of some models of myelinated axons, IMA Journal of Mathematics Applied in Medicine and Biology, 1 (1984), 149–167.

[4] J. Bell and C. Cosner, Threshold conditions for a diffusive model of a myelinated axon, J. Math. Biology, 18 (1983), 39–52.

[5] H. Chi, J. Bell and B. Hassard, Numerical solution of a nonlinear advance-delay-differential equation from nerve conduction theory, J. Math. Biol., 24 (1986), 583–601.

[6] C.E. Elmer and E. Van Vleck, A variant of Newton's method for the computation of traveling waves of bistable differential-difference equations, J. Dyn. Dif. Eqn., 14 (2002), 493–517.

[7] P.C. Fife and J.B. McLeod, The approach of solutions of nonlinear diffusion equations to travelling wave solutions, Arch. Rational Mech. Anal., 65 (1977), 33–361.

[8] R. FitzHugh, Impulses and physiological states in theoretical models of nerve membrane, Biophysical J., 1(1961), 445–466.

[9] R. FitzHugh, Computation of impulse initiation and saltatory condition in a myelinated nerve fiber, Biophysical J., 2 (1962), 11–21.

[10] H. Fu, L. Wan, Y. Wang, and J. Liu, Strong convergence rate in averaging principle for stochastic FitzHugh-Nagumo system with two time-scales, J. Math. Anal. Appl., 416 (2014), 609–628.

[11] A. Hodgkin and A. Huxley, A qualitative description of nerve current and its application to conduction and excitation in nerve, J. Physiology, 117 (1952), 500–544 .

[12] H.J. Hupkes and S.M. Verduyn Lunel , Analysis of Newtons method to compute travelling waves in discrete media, J. Dyn. Dif. Eqn., 17 (2005), 523–571.

[13] J.P. Keener, Propagation and its failure in coupled systems of discrete excitable cells, SIAM J. Appl. Math., 47 (1987), 556–572.

[14] P.M. Lima, M.F. Teodoro, N.J.Ford, P. M.Lumb, Analysis and Computational Approximation of a Forward-Backward Equation Arising in Nerve Conduction,in Differential and Difference Equations with Applications, Springer Proceedings in Mathematics and Statistics, Volume 47, 2013, pp 475-483.

[15] J. Mallet-Paret, The global structure of traveling waves in spattially discrete dynamical systems, J. Dyn. Dif. Eqn., 11, 1 (1999), 49–128.

[16] D.R. McNeal, Analysis of a model for excitation of myelinated nerve, IEEE Transactions on Biomedical Engineering, 23 (1976) , 329–337.

[17] J. Nagumo, S.Arimoto and S. Yoshizawa, An active pulse transmission line simulating nerve axon, Proceedings of the IRE, 50 (1962), 2061–2070.

[18] H. Namazi and V. Kulish, A mathematical based calculation of a myelinated segment in axons, Computers in Biology and Medicine, 43 (2013), 693–698.

[19] J.Rinzel and J.B. Keller, Travelling wave solutions of a nerve conduction equation, Biophysical J., 13 (1973), 1313–1337.

[20] J. Rinzel, Spatial stability of travelling wave solutions of a nerve conduction equation, Biophysical J., 15 (1975), 975–988.

[21] S. Wolfram, *The Mathematica Book. Wolfram Media, fifth ed.*, 2003.

[22] C. Zanini and F. Zanolin, Multiplicity of periodic solutions for differential equations arising in the study of a nerve fiber model, Nonlinear Analysis, Real World Applications, 9 (2008), 141-153.

[23] B. Zinner, Stability of travelling wavefronts for discrete Nagumo Equation, SIAM J. of Math. Anal., 22 (1991), 1016–1020.